PHYSICAL REVIEW B **72**, 081310(R) (2005)

Direct control of the tunnel splitting in a one-electron double quantum dot

A. K. Hüttel,[1] S. Ludwig,[1] H. Lorenz,[1] K. Eberl,[2] and J. P. Kotthaus[1]
[1]*Center for NanoScience and Department für Physik, Ludwig-Maximilians-Universität, Geschwister-Scholl-Platz 1, 80539 München, Germany*
[2]*Max-Planck-Institut für Festkörperforschung, Heisenbergstraße 1, 70569 Stuttgart, Germany*
(Received 7 June 2005; published 24 August 2005)

Quasistatic transport measurements are employed on a laterally defined tunnel-coupled double quantum dot. A nearby quantum point contact allows us to track the charge as added to the device. If charged with only up to one electron, the low-energy spectrum of the double quantum dot is characterized by its quantum mechanical interdot tunnel splitting. We directly measure its magnitude by utilizing particular anticrossing features in the stability diagram at finite source-drain bias. By modification of gate voltages defining the confinement potential, as well as by variation of a perpendicular magnetic field, we demonstrate the tunability of the coherent tunnel coupling.

DOI: 10.1103/PhysRevB.72.081310 PACS number(s): 73.21.La, 73.20.Jc, 73.23.Hk

Recent works have shown spectacular advancements regarding the control over single electrons trapped in semiconductor-based quantum dots (QD).[1–4] Electronic states in separate QDs can be coupled, resulting in delocalized and spatially coherent "molecular modes."[5–8] QDs thus lend themselves as prospective building blocks for qubits, the elementary units of the proposed quantum computer. Models for QD-based qubits include, e.g., the use of a single electronic spin in one QD.[9,10] Alternatively, the position of a single electronic charge within a double quantum dot (DQD) has been proposed.[11] For both approaches, precise control of the coupling between nearby QDs is of paramount importance. We report on quasistatic measurements allowing direct determination of the interdot tunnel splitting of a strongly coupled DQD charged with up to one electron. Control over the tunnel coupling via gate voltages or magnetic field is demonstrated.

Our measurements are performed using an epitaxial AlGaAs/GaAs heterostructure that forms a two-dimensional electron system (2DES) 120 nm below the crystal surface with a carrier sheet density of $n_s = 1.8 \times 10^{15}$ m^{-2} and an electron mobility of $\mu = 75$ m^2/V s, both measured at 4.2 K. The 2DES temperature is estimated to be $T_{2DES} \simeq 100$ mK. We use a lock-in frequency of 840 Hz (Fig. 1) or 680 Hz (Figs. 3 and 4).

Figure 1(a) displays an electromicrograph of the gates on the surface of our heterostructure. Application of negative dc voltages to these electrodes allows definition of a DQD as well as a quantum point contact (QPC) in the 2DES. Our layout is based on a gate geometry introduced by Ciorga *et al.*[2] It allows a measurable single electron tunneling (SET) current through the QD even in the limit of only one trapped electron. To elongate a single QD and split it into a double well potential we increase the absolute values of the dc voltages $|U_{gC}|$ and $|U_{gX}|$ of the center gates [cf. Fig. 1(a)]. To keep the overall charge of the system constant, we decrease $|U_{gL}|$ and $|U_{gR}|$ on the side gates. The approximately resulting serial DQD is sketched in Fig. 1(a) in a bright tone.

The stability diagram in Fig. 1(b) displays the differential transconductance $G_{QPC} = dI_{QPC}/dU_{gL}$ through the nearby QPC in dependence on the dc voltages applied to gates g_L and g_R. The QPC serves as a charge sensor, as described in Refs. 12 and 13. The darker lines in the plot depict reduced transconductance corresponding to discrete charging events in the DQD while otherwise the electron number in the DQD is constant. These lines clearly form a honeycomb structure as expected for a DQD.[14–16] The lack of charging events in the area marked by 0/0 in Fig. 1(b) implies that here our DQD is free of extra charges. Note that this area is bordered on its upper and right side by a distinct line of low transconductance proving that our resolution is high enough to detect all charging events for the shown gate voltages. We mark the area of the plot for which only the right QD is charged by one electron with 0/1, for which one electron is trapped in each QD with 1/1, and so on. The smooth charge redistribution from configuration 0/1 to 1/0 contrasts results for weak interdot coupling.[14,17] A second hint at strong coupling is the lack of sharp corners of the lines of reduced transconductance at triple points in the stability diagram, where three charge configurations are possible.

The open circles in Fig. 1(b) depict local maxima of cur-

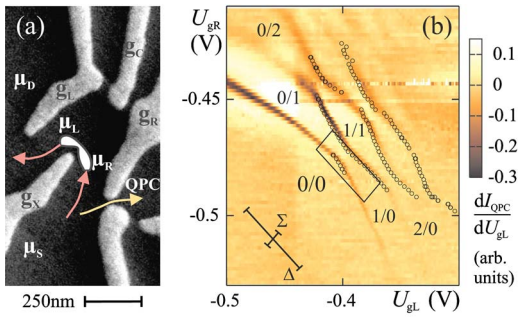

FIG. 1. (Color online) (a) Scanning electron microscopy image of the gate electrodes used for defining a DQD and a QPC. The approximate geometry of the DQD (white area) and electron flow (arrows) are indicated. (b) Stability diagram of the DQD plotting the transconductance dI_{QPC}/dU_{gL} through the QPC. A background signal has been subtracted. The open circles indicate local maxima of current through the DQD at constant U_{gR}. The bars (Σ, Δ), each corresponding to 1 meV, illustrate the axis directions, the box the plot range of Figs. 2 and 3.

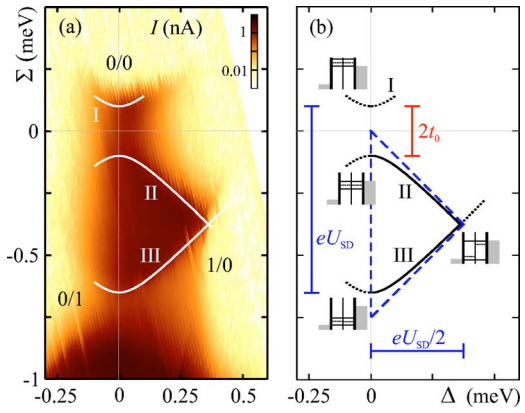

FIG. 2. (Color online) (a) Measurement of the SET current through a one-electron DQD at $U_{SD}=-0.75$ mV and $U_{gC}=-1.47$ V (logarithmic scale), including model lines for strong interdot coupling [see (b)]. (b) Corresponding model expectations for SET transport features at finite source-drain bias in the two cases of weak (dashed lines) versus strong (solid and dotted lines) interdot coupling.

rent I_{DQD} through the serial DQD at constant U_{gR}, recorded in linear response ($U_{SD}=50$ μV). For weak interdot coupling we expect a finite current through this system only at triple points in the stability diagram. In contrast, we also find current along parts of the configuration boundaries away from triple points. This suggests that the electron can lower its orbital energy by forming a delocalized state, as well indicating strong interdot tunnel coupling. The configuration boundaries obtained show excellent agreement with the QPC measurement. For more than two trapped electrons, coupling to the leads results in current line broadening; then some phase boundaries cannot be resolved as separate maxima anymore. Note that we can perform direct current measurements through the DQD even if it is charged with only up to one electron.

Starting from the limit of a weakly coupled DQD we will now outline a model including coherent interdot tunnel coupling, describing the static transport properties at finite source-drain bias. Comparison with measurements demonstrates our ability to detect and tune the tunnel splitting of the single electron states in a DQD.

Figure 2(a) displays the SET current through the DQD for the region of the stability diagram framed in Fig. 1(b) by a rhomboid, but measured at a source-drain bias of $U_{SD}=-0.75$ mV. Here, we use a transformed coordinate system reflecting the symmetry properties of the DQD. The chemical potentials of the QDs marked in Fig. 1(a) as μ_L and μ_R are defined as the energies required to add the first electron to the respective QD. Our x axis measures the interdot asymmetry $\Delta\equiv(\mu_R-\mu_L)/2$, while the y axis plots the average chemical potential of both QDs $\Sigma\equiv(\mu_R+\mu_L)/2$. Direction and scale of these axes, indicated in Fig. 1(b) by two black bars, reflect the capacitances between QDs and gate electrodes.[15,16]

Narrow current features in the stability diagram at zero source-drain bias expand to regions of finite current for $|U_{SD}|>0$ as displayed in Fig. 2(a). Here $\mu_D<\mu_S$ and for weak interdot coupling the condition $\mu_D\leqslant\mu_L\leqslant\mu_R\leqslant\mu_S$ defines a triangular region of finite SET current illustrated in Fig. 2(b) by dashed lines.[3,15] The triangle baseline is located on the Σ axis where $\mu_L=\mu_R$. The other two edges have slopes $d\Sigma/d\Delta=\pm1$ corresponding to either $\mu_R=\mu_S$ or $\mu_L=\mu_D$. They meet at the tip of the triangle with $2\Delta=\mu_S-\mu_D\equiv|eU_{SD}|$, where e is the electron charge. The transformation from the coordinates in Fig. 1(b) to those in Fig. 2 is based on the geometry of this triangle and on the comparison to a reference energy scale provided by $|eU_{SD}|$.

The SET current measurement plotted in Fig. 2(a) illustrates a strong interdot coupling situation, where the electronic ground states of the two QDs hybridize into delocalized states. At $\mu_L=\mu_R$ the corresponding chemical potentials μ_+ of the symmetric ground state and μ_- of the antisymmetric excited state are separated by the tunnel splitting $2t_0$. For finite interdot asymmetry Δ this energy splitting becomes $\sqrt{(2\Delta)^2+(2t_0)^2}$.

The resulting expected edges of strong (weak) current onset are indicated as solid (dotted) model lines in Figs. 2(a) and 2(b). Level schemes in Fig. 2(b) sketch the alignment of μ_+ and μ_- compared to the lead chemical potentials μ_S and μ_D at nearby intersection points of these lines and the Σ axis. For the DQD containing up to one electron, SET is possible in a region spanned by lines I and III. A first conductance channel opens at line I where $\mu_+=\mu_S$, and a second at $\mu_-=\mu_S$ (II). The Coulomb blockade suppresses the current for $\mu_+<\mu_D$ (III). Thus, the fourth possible alignment, $\mu_-=\mu_D$, does not appear as current change. Model lines I and II result in an anticrossing at $\Delta=0$ with tunnel splitting $2t_0=|\mu_--\mu_+|$.

At even smaller values of Σ, below line III in Fig. 2(a), the region of high current (dark area) corresponds to the onset of the DQD being charged with a second electron. Here, Coulomb repulsion and exchange interaction have to be taken into account, causing a different energy spectrum. The in comparison to the background slightly darker graytone in the region $0\lesssim2\Delta\lesssim|eU_{SD}|$ below line III indicates a small cotunneling current.

Between lines I and II the excited state of the DQD is permanently unoccupied since $\mu_->\mu_S$. SET is only possible through the delocalized symmetric ground state. In Fig. 2(a) we observe current only for small asymmetry $|\Delta|\lesssim t_0$ between lines I and II. With increasing asymmetry the ground state is more and more localized in one of the QDs and current vanishes for $|\Delta|\gg t_0$. A smaller signal for negative than for positive asymmetry is detected. This broken symmetry hints at a larger tunnel barrier of the DQD towards its drain contact compared to that on its source side. In contrast, between lines II and III both electron states with chemical potentials μ_+ and μ_- contribute to the current. Here, for $\Delta<0$ energy relaxation from the left to the right QD competes with the tunnel rate into drain, hindering the SET current through the DQD. For $\Delta\ll0$ localization of the ground state in the right QD near the source contact causes Coulomb blockade.

In the region spanned by lines II, III, and the Σ axis we observe a strong current signal. Here, the chemical potentials obey $\mu_S\geqslant\mu_-\geqslant\mu_+\geqslant\mu_D$. For small asymmetry, SET through both then delocalized states contributes to the current. As the asymmetry Δ and thereby localization of the two states in the

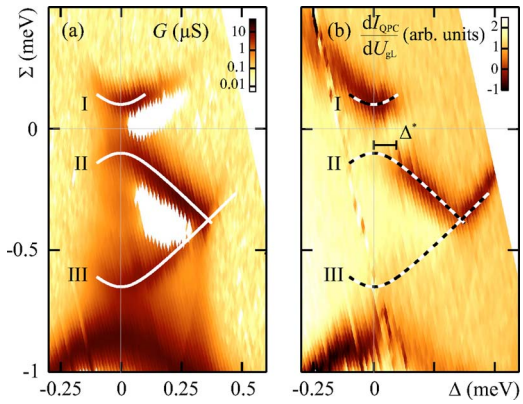

FIG. 3. (Color online) (a) Differential conductance $dI_{\mathrm{DQD}}/dU_{\mathrm{SD}}$ through the DQD corresponding to the current measurement shown in Fig. 2(a) (identical parameters, logarithmic scale). (b) The corresponding differential transconductance $dI_{\mathrm{QPC}}/dU_{\mathrm{gL}}$ through a nearby QPC (linear scale). For both plots, the model lines are identical to those in Fig. 2.

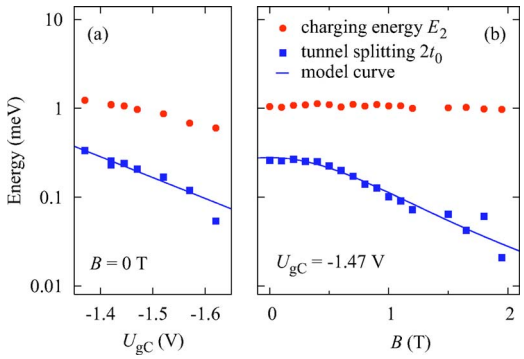

FIG. 4. (Color online) (a) Tunnel splitting $2t_0$ of the one-electron DQD and charging energy for the second electron E_2 in dependence on gate voltage U_{gC}. (b) E_2 and $2t_0$ plotted as function of a perpendicular magnetic field.

two separate QDs increases, direct SET through each of these states is suppressed. For $\Delta \gg t_0$ the electronic states of the DQD can be approximated by the two single QD ground states with $\mu_- \simeq \mu_{\mathrm{R}}$ and $\mu_+ \simeq \mu_{\mathrm{L}}$. In this configuration, resembling the weak coupling limit, an electron can hop through the double dot starting from the source contact via the right to the left dot and finally to drain, losing energy between the two dots.[18] This additional energy relaxation process impedes SET and causes a decrease in total current.

Figure 3(a) displays the corresponding differential conductance $dI_{\mathrm{DQD}}/dU_{\mathrm{SD}}$ in the logarithmic scale. The tunnel splitting $2t_0$, visible as the anticrossing of lines I and II, is here even more obvious than in the current measurement. Note that the model lines in all Figs. 2 and 3 are identical. The regions of negative differential conductance (NDC), plotted in white, reflect the dependence of tunnel and relaxation rates on U_{SD}. We find that localization increases with growing U_{SD}, in turn causing a slower energy relaxation between the localized QDs. While this scenario explains NDC between lines II and III, for the NDC area above line II in addition higher order tunnel processes have to be considered involving the excited state with $\mu_- > \mu_{\mathrm{S}}$.

In Fig. 3(b) the differential transconductance of the QPC $dI_{\mathrm{QPC}}/dU_{\mathrm{gL}}$ is plotted for the same area of the stability diagram as the measurements discussed above. The resonances of small signal (dark areas) are caused by changes of the time-averaged charge inside the DQD.[13,14] They follow parts of our model lines already shown in Figs. 2 and 3. The dark area at the lower plot edge reflects the onset of charging the DQD with a second electron. Above this area for each distinct asymmetry value Δ only a single charging resonance is observed (the splitted dark feature). Thus, at this resonance the charge of the DQD almost discretely switches between zero and one electron. For $\Delta \lesssim 0$ charging takes place at the first possible alignment of the chemical potentials of the DQD and the source contact ($\mu_+ \simeq \mu_{\mathrm{S}}$ at model line I). At a finite asymmetry $\Delta^* > 0$, indicated in Fig. 3(b), this measured resonance jumps to line II with $\mu_- \simeq \mu_{\mathrm{S}}$, where a second transport channel opens. The jump at $\Delta^* > 0$ provides information on the rates of an electron entering and escaping the DQD, suggesting a larger tunnel barrier towards the drain than the source contact. For $\mu_- > \mu_{\mathrm{S}}$, the rates are identical at $\Delta = \Delta^*$. At $\Delta < \Delta^*$ an electron tunnels faster into the ground state of the DQD than it escapes to the drain contact. For $\Delta > \Delta^*$ the escape rate dominates and the DQD stays mostly empty at line I. This larger escape rate is caused by increasing localization of the DQD ground state in the QD near the drain contact as Δ grows positive. Note that the asymmetric current along line I allows the same interpretation.

At $\mu_- \simeq \mu_{\mathrm{S}}$ (line II) another channel via the excited state opens. The tunnel rate into this state is large, since for $\Delta > 0$ it is predominantly localized near the source contact. In comparison, for $\Delta > t_0$ the escape rate is limited by the product of the relaxation rate between the partly localized QDs and the tunnel rate from the left QD to the drain reservoir. Thus, below line II the DQD average charge is approximately one electron. For $2\Delta > |eU_{\mathrm{SD}}|$, the charging resonance follows line III featuring $\mu_+ \simeq \mu_{\mathrm{D}}$, where the DQD enters Coulomb blockade.

Figure 4 plots the tunnel splitting $2t_0$, and the charging energy E_2 required to add a second electron to the DQD as a function of center gate voltage U_{gC} (a) and perpendicular magnetic field (b). E_2 is obtained as the energy difference between the onset of current involving one compared to two electrons in a symmetric DQD, e.g., from Fig. 3(a) as the distance between line I and the center of the dark line at the bottom of the plot. As we separate the two QDs more by increasing the interdot tunnel barrier [Fig. 4(a)], both $2t_0$ and E_2 decrease. In contrast, with growing magnetic field only $2t_0$ decreases considerably while E_2 stays almost unaltered. Note that E_2 primarily depends on the distance of the centers of charge of both QDs. In comparison, the tunnel rate is additionally influenced by the potential geometry governing the overlap of the single QD states. Clearly, U_{gC} alters the electrostatic potential geometry whereas B mainly leads to a compression of the electronic states at almost constant mean distance, leaving $E_2(B)$ unchanged.

Using the WKB method the tunnel splitting of the DQD is found to be approximately $2t_0 \simeq 2E_0/\pi \exp(-\sqrt{2m^*\Phi}d/2\hbar)$, where E_0 is the mean ground state energy of both QDs, m^* the effective electron mass, and where d and Φ are the ef-

fective width and amplitude of a quartic tunnel barrier potential. An exponential decrease of $2t_0$ at increasing $|U_{gC}|$, as indicated by a solid line in Fig. 4(a), suggests a nearly linear increase of $\sqrt{\Phi}d$.

Figure 4(b) displays $2t_0$ and E_2 at a fixed voltage $U_{gC}=-1.47$ V in dependence of magnetic field B. The tunnel splitting remains constant at $2t_0 \simeq 260$ μeV for $B \lesssim 0.4$ T, but decreases for stronger B. At constant mean distance, we assume each QD to extend over the Fock-Darwin length scale[1,19] $l_{QD}(B) \equiv \sqrt{\hbar/\omega_c m^*}/\sqrt[4]{1+4\Omega^2/\omega_c^2}$. Here Ω characterizes the parabolic confinement and $\omega_c = eB/m^*$. The WKB formula then results in a model curve (solid line) showing qualitative good agreement with our data. For a quantitative analysis the actual overlap of the wave functions within a realistic potential had to be considered.

In conclusion, we have directly observed the coherent quantum mechanical interdot tunnel coupling of a one-electron DQD employing quasistatic transport measurements. At finite source-drain bias the delocalized electronic eigenstates of the strongly coupled DQD generate a distinct pattern in the stability diagram visible in current, conductance, and average charge on the DQD. In all three quantities, the tunnel splitting is immediately visible as a clear anticrossing and can be quantified after a coordinate transformation. To tune the tunnel splitting we modify gate voltages or a magnetic field perpendicular to the 2DES. We propose a simple model and find our data in qualitative agreement.

We thank R. H. Blick, U. Hartmann, and F. Wilhelm for valuable discussions, and S. Manus for expert technical help, as well as the Deutsche Forschungsgemeinschaft QIV and the BMBF for support. A. K. H. thanks the German National Academic Foundation for support.

[1] L. P. Kouwenhoven, D. G. Austing, and S. Tarucha, Rep. Prog. Phys. **64**, 701 (2001).
[2] M. Ciorga, A. S. Sachrajda, P. Hawrylak, C. Gould, P. Zawadzki, S. Jullian, Y. Feng, and Z. Wasilewski, Phys. Rev. B **61**, R16315 (2000).
[3] A. C. Johnson, J. R. Petta, C. M. Marcus, M. P. Hanson, and A. C. Gossard, cond-mat/0410679 (unpublished).
[4] R. Hanson, L. M. K. Vandersypen, L. H. Willems van Beveren, J. M. Elzerman, I. T. Vink, and L. P. Kouwenhoven, Phys. Rev. B **70**, 241304(R) (2004).
[5] R. H. Blick, D. Pfannkuche, R. J. Haug, K. v. Klitzing, and K. Eberl, Phys. Rev. Lett. **80**, 4032 (1998).
[6] A. W. Holleitner, R. H. Blick, A. K. Hüttel, K. Eberl, and J. P. Kotthaus, Science **297**, 70 (2002).
[7] T. Hayashi, T. Fujisawa, H. D. Cheong, Y. H. Jeong, and Y. Hirayama, Phys. Rev. Lett. **91**, 226804 (2003).
[8] T. Hatano, M. Stopa, T. Yamaguchi, T. Ota, K. Yamada, and S. Tarucha, Phys. Rev. Lett. **93**, 066806 (2004).
[9] D. Loss and D. P. DiVincenzo, Phys. Rev. A **57**, 120 (1998).
[10] L. M. K. Vandersypen, R. Hanson, L. H. Willems van Beveren, J. M. Elzerman, J. S. Greidanus, S. De Franceschi, and L. P. Kouwenhoven, in *Quantum Computing and Quantum Bits in Mesoscopic Systems*, edited by A. Leggett, B. Ruggiero, and P. Silvestrini (Kluwer Academic, New York, 2004).
[11] W. G. van der Wiel, T. Fujisawa, S. Tarucha, and L. P. Kouwenhoven, Jpn. J. Appl. Phys., Part 1 **40**, 2100 (2001).
[12] M. Field, C. G. Smith, M. Pepper, D. A. Ritchie, J. E. F. Frost, G. A. C. Jones, and D. G. Hasko, Phys. Rev. Lett. **70**, 1311 (1993).
[13] D. Sprinzak, Yang Ji, M. Heiblum, D. Mahalu, and H. Shtrikman, Phys. Rev. Lett. **88**, 176805 (2002).
[14] J. M. Elzerman, R. Hanson, J. S. Greidanus, L. H. Willems van Beveren, S. De Franceschi, L. M. K. Vandersypen, S. Tarucha, and L. P. Kouwenhoven, Phys. Rev. B **67**, 161308(R) (2003).
[15] W. G. van der Wiel, S. De Franceschi, J. M. Elzerman, T. Fujisawa, S. Tarucha, and L. P. Kouwenhoven, Rev. Mod. Phys. **75**, 1 (2003).
[16] F. Hofmann, T. Heinzel, D. A. Wharam, J. P. Kotthaus, G. Böhm, W. Klein, G. Tränkle, and G. Weimann, Phys. Rev. B **51**, 13872 (1995).
[17] J. R. Petta, A. C. Johnson, C. M. Marcus, M. P. Hanson, and A. C. Gossard, Phys. Rev. Lett. **93**, 186802 (2004).
[18] T. Fujisawa, T. H. Oosterkamp, W. G. van der Wiel, B. W. Broer, R. Aguado, S. Tarucha, and L. P. Kouwenhoven, Science **282**, 932 (1998).
[19] V. Fock, Z. Phys. **47**, 446 (1928).